Quantitative Analysis of Electron Field-Emission Characteristics of Individual Carbon Nanotubes: The Importance of the Tip Structure

M. S. Wang,[†] L.-M. Peng,*[,†] J. Y. Wang,[†] C. H. Jin,[‡] and Q. Chen[†]

Key Laboratory for the Physics and Chemistry of Nanodevices and Department of Electronics, Peking University, Beijing 100871, China, and National Laboratory on Condensed Matter Physics, Institute of Physics, Chinese Academy of Sciences, P.O. Box 603, Beijing 100080, China

Received: September 2, 2005; In Final Form: February 7, 2006

Electron field-emission measurements on individual carbon nanotubes (CNTs) were performed inside the transmission electron microscope (TEM). The field-emission characteristics of CNTs with different tip structures were compared, and their field conversion factor and emission area were studied systematically. It was found that the field-emission characteristics of a CNT depend sensitively on its tip structure, and in particular an opened CNT was shown to be superior to a capped CNT. High-resolution TEM observations revealed that the tip of an opened CNT may, in general, be regarded as being composed of irregular shaped graphitic sheets, and these graphitic sheets have been found to improve dramatically the field-emission characteristics, but the sharp edge may result in larger error in the calculated emission area. The influence of uncertainty in the work function of the CNTs on the field conversion factor and emission area calculation was also investigated.

I. Introduction

Among the many possible applications of carbon nanotubes (CNTs),[1] the most promising one is perhaps to use CNTs as field-emission electron source,[2−4] especially for flat field-emission displays,[3,4] and many people believe that CNTs could oust plasma in big-screen televisions.

Although impressive progress has been made in recent years it is still not fully understood as to how the morphology of the CNT affects its field-emission characteristics. Bonard et al.[5] studied the dependence of the field enhancement with inter-electrode distance, radius, and length of individual CNTs inside scanning electron microscopy (SEM) and showed that only a small part of exceptionally long and/or narrow nanotubes contributes to the emitted current in large area measurements. However, there existed significant difference between their experimental data and the calculated values using the Edgcombe and Valdre model, and they believed that these results show that the emission process is highly sensitive to the exact tip structure.[5,6] In fact, it has been realized from the first studies on the field emission of a CNT that the emission current depends sensitively on the structure of the CNT and in particular the current was enhanced dramatically when the nanotube tips were opened by laser evaporation or oxidative etching.[7] It was proposed that the enhancement on the emission was due to linear chains of carbon atoms, pulled out from the open edges of the graphene wall layers of the CNT. However, this unraveling process was not confirmed experimentally, and indeed was later rejected by Saito et al.[8] based on their field-emission microscope (FEM) observations. Instead it was concluded that electron emission results from the circular edges of the graphitic layers of the CNT. Recently, structure damage during field emission has been observed in situ inside the transmission electron microscope (TEM)[9,10] and the work function at the nanotube tip has been found to depend strongly on its structure and surface condition.[11] But until now a systematical study on how the tip structure affects the field-emission characteristics is still lacking.

Here we present a field-emission measurement on individual CNTs inside the TEM. All CNT emitters were created by precise manipulation of individual CNTs inside the TEM. The tip structures can be modified by some controllable processes, and at the same time, other parameters such as the interelectrode distance and the length and diameter of the CNT can be obtained precisely by TEM imaging, and these parameters were found to hardly change during our experiments. These highly controlled experiments therefore allow us to compare directly the field-emission properties of different tip structures. In particular, we show that in general the emitting tip of an opened CNT may be regarded as being composed of graphitic sheets of irregular shape instead of circular edge, and it is these irregular-shaped graphitic sheets exposed to the strongly enhanced local field at the tip that make the opened CNTs such good field emitters.

II. Experimental Section

In a typical experiment, two metal electrodes were used for measuring the electron field-emission current. The first electrode was a microscopically flat Pt tip that was prepared by simply cutting a pure Pt wire of 0.25 mm using a scissor. The second electrode was a very sharp W-tip (typically with a radius of curvature of about 20 nm) that was prepared using the standard electrochemical etching method. To remove the thin oxide layer from the surface of the W-tip and therefore to improve the electric conductivity of the tip, the W-tip was first moved into contact with the Pt-tip inside the TEM. The sharp W-tip was readily melted on passing a large current through the tips, resulting in a clean W-tip with a slightly larger radius. All of the CNTs used in this study were multiwalled CNTs (MWCNTs) prepared by chemical vapor deposition (CVD). The CNTs were assembled onto the Pt tip before each experiment by rubbing the Pt-tip in nanotube powder. The microscopically flat Pt-tip was kept stationary while individual CNTs were selected by the sharp W-tip inside the TEM. A 200 kV TEM (Tecnai

* To whom correspondence should be addressed. E-mail: lmpeng@pku.edu.cn.
[†] Peking University.
[‡] Chinese Academy of Sciences.

10.1021/jp054971i CCC: $33.50
Published on Web 04/26/2006

G20) and a single-tilt TEM sample holder (Nanofactory)[10,12] integrated with a scanning tunneling microscope (STM) was used in this work. The W-tip was connected to a piezotube that allows a fine movement of the W-tip in three dimensions over several micrometers, and the piezo resolution for the movement is better than 0.02 nm in all directions. The vacuum level in the TEM was 1×10^{-5} Pa. A large field-emission current of 10−20 μA (a larger current may cause damage of the tip structure[10] or even catastrophic arcs[12]) was extracted to heat the nanotube by applying a constant voltage. This heating process[13] usually lasts for 10 s, and we believe complication due to adsorbates was minimized via this procedure. After the heating, the field-emission measurement was immediately carried out. Up to 140 V may be applied between the two metal tips, and the acquisition time for each $I-V$ sweep cycle with 200 data points was set to 200 ms. Every field-emission current voltage ($I-V$) curve presented in this paper was an average of typically 10−50 $I-V$ sweep cycles.

III. Results and Discussions

The goal of correlating field-emission characteristics of CNTs with their structures has been pursued actively since the first report on electron field emission from individual CNTs by Rinzler et al.[7] Specially built apparatus for field-emission measurements have been introduced into both TEM and SEM. Although many valuable results have been obtained, the measured field-emission characteristics were yet to be related directly to the detailed structural features of the CNT tips. The main obstacle for a reliable systematic investigation on the tip structure and field-emission property relationship is the controlled preparation of different tip structures, and in this study we employed the method as demonstrated in Figure 1.

A cleaned (i.e., melted) W-tip was first moved to contact with a MWCNT with a bamboo structure protruding form the edge of the top Pt electrode (Figure 1a, but the top Pt electrode was not shown). The total resistance of the two-terminal $I-V$ measurement was reduced to several tens of kiloohms by current annealing.[14] In our experiments the CNTs have a diameter of about 20−40 nm. These large CNTs may be practically regarded as metallic at room temperature and usually make good ohmic contact with the electrodes. A new capped CNT tip was pulled out from the old one (Figure 1a and b). Amorphous carbon (a-C) may be deposited at the contact point, for example, with the W-tip via an electron-beam-induced deposition process[14] prior to the above pulling process to pin the CNT to the electrode. This freshly created capped CNT was then moved to a place where the counter Pt electrode was flat and can be used as the anode for the field-emission experiment (Figure 1c). After the measurement, the capped nanotube was moved to touch the counter electrode with a bias of 4 V and a current limited below 50 μA (Figure 1d) and the cap of the nanotube was removed (Figure 1e). The nanotube was shortened by about 4 nm, leaving a flat opened end (Figure 1e). The W-tip was then retracted to its original place for field-emission measurement (Figure 1f). The field-emission $I-V$ curves were presented in Figure 1g, and the corresponding Fowler−Nordheim (F−N) plots were obtained by plotting $\ln(I/V^2)$ verses $1/V$ and shown in Figure 1h.

A standard form of the F−N equation[15] is

$$J = (a/\phi t(y)^2)\, F^2 \exp(-b\phi^{3/2} v(y)/F) \qquad (1)$$

where J is current density, a and b are universal constants given by[16] $a = 1.541434 \times 10^{-6}$ A eV V^{-2}, $b = 6.830888 \times 10^9$ eV$^{-3/2}$ V m^{-1}, ϕ is the work function of the electron emitter, F

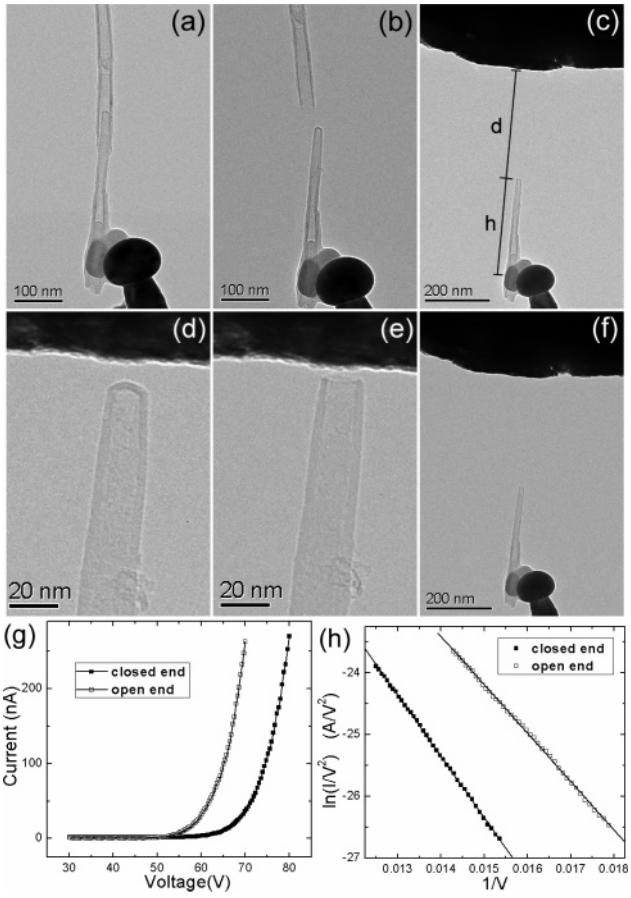

Figure 1. TEM images showing a CNT with a bamboo structure (a), and a capped CNT tip being pulled out from the CNT (b). The capped CNT tip was then moved to face a flat counter top Pt electrode for field-emission measurements (c). To modify the tip structure of the CNT, the CNT was moved to a position that was very close to the counter electrode (d) and the cap was removed by electrically-driven vaporization (e). The freshly opened nanotube was then retracted to original place for future field-emission measurements (f). The $I-V$ curves and corresponding F−N plots for capped and opened CNTs are shown in g and h, respectively.

$= \beta V$ (β being the field conversion factor), $y = cF^{1/2}/\phi$ with $c = 3.794687 \times 10^{-5}$ eV V$^{-1/2}$ m$^{1/2}$, and $t(y)$ and $v(y)$ are two functions of y (see below). Assuming $I = JA$, with A being the emission area, we obtain

$$\ln(I/V^2) = \ln(Aa\beta^2/\phi t^2) - b\phi^{3/2} v(y)/\beta V \qquad (2)$$

Because $t(y)$ is a slowly varying function of the field at the tip, the field dependence of $\ln(t^{-2})$ can be assumed to be negligible. The slope of the F−N plot, S, is thus given by[17]

$$S = \mathrm{d}(\ln(I/V^2))/\mathrm{d}(1/V) = -(b\phi^{3/2}/\beta)s(y) \qquad (3)$$

with

$$s(y) = v(y) - (y/2)(\mathrm{d}v/\mathrm{d}y), \qquad (4)$$

and

$$\beta = -b\phi^{3/2}\mathrm{s}(y)/S \qquad (5)$$

Recently, Forbes gave a general expression relating the emission area, A, to the intercept of the experimental F−N plot, R (see eq 11 of ref 16)

$$R = \ln(Aa\beta^2/\phi t^2) - b\phi^{3/2}(\mathrm{d}v/\mathrm{d}F)_{V_0} \qquad (6)$$

TABLE 1: Measured and Calculated Parameters Relevant to Electron Field-Emission for Some Typical Samples

sample no.	S	R	V_0 (V)	d (nm)	h (nm)	r (nm)	$1/\beta$ (nm)	V_{onset} (V)	F_{onset} (V/nm)	A (nm^2)	$1/\beta^{CM}$ (nm)	A^{CM} (nm^2)
1 (Figure 1d)	−990.7	−11.48	72.56	324	301	8.0	13.75	57.15	4.16	79.97	13.57	62.94
2 (Figure 1e)	−782.9	−12.45	62.96	325	297	8.0	10.92	48.78	4.47	20.45	10.72	14.92
3 (Figure 2a)	−1378.1	−10.99	92.46	875	1156	16.1	19.05	75.03	3.94	234.54	18.87	198.32
4 (Figure 2b)	−917.0	−10.41	63.49	878	1082	14.0	12.70	50.49	3.98	191.66	12.56	157.95
5 (Figure 2c)	−895.8	−12.50	71.56	486	671	13.8	12.49	55.14	4.42	25.39	12.27	18.62
6 (Figure 2d)	−1195.7	−12.45	90.70	486	626	17.3	16.63	71.18	4.28	45.26	16.38	34.61
7 (Figure 3a)	−528.5	−8.32	32.98	239	124	10.4	7.28	27.75	3.81	470.08	7.24	421.82
8 (Figure 3b)	−1046.3	−10.34	71.36	262	101	10.4	14.47	56.70	3.92	262.24	14.33	218.80
9 (Figure 3c)	−464.3	−13.07	41.58	943	928	1.7	6.51	31.85	4.89	4.23	6.36	2.82
10 (Figure 3d)	−912.5	−9.74	61.53	969	902	11.3	12.62	48.66	3.86	360.96	12.50	303.96

where $v(y)$ and $t(y)$ are tabulated function of y and may be approximated as $v(y) = 1 - y^{1.69}$ and $t(y) = 1 + 0.1107y^{1.33}$ (by Hawkes and Kasper,[6,18] and we call it the HK approximation in our following discussion). Substitution of these expressions into eqs 4−6 gives

$$s(y) = 1 - 0.015y_0^{1.69} \tag{7}$$

$$\beta = -b\phi^{3/2}(1 - 0.155y_0^{1.69})/S \tag{8}$$

and

$$R = \ln[Aa\beta^2/\phi(1 + 0.1107y_0^{1.33})^2] + b\phi^{3/2}(0.845y_0^{1.69}/\beta V_0) \tag{9}$$

For a CNT we take $\phi = 5$ eV and evaluate V_0 at the middle of the effective voltage range. Experimental $I-V$ data within this voltage range were used in evaluating the F−N plot, giving

$$y_0 = c(\beta V_0)^{1/2}/\phi \tag{10}$$

We first set $\beta = -b\phi^{3/2}/S$ and then use eqs 10 and 8 to calculate the values of β and y_0 accurately by iterative approach. The emission area, A, can be obtained using the so obtained β and y_0 from the experimental F−N plot and using eq 9.

The accuracy in our current measurement is about 1 nA, which may lead to larger error in F−N plot when the current is below 10 nA. A large current range may lead to a change in the effective emission area, and a very large current density can sometimes lead to a deviation of the F−N plot from a perfect linear relation due to, for example, current heating[13] or structure change. So the data in the F−N plot are limited within the current range from 10 nA to several hundred nanoamperes, and we found that in this range a good linear F−N plot can usually be obtained. People always use 1 nA as the reference for the onset voltage. Because it is difficult for us to obtain this value experimentally, we calculated this onset voltage by fitting the experimental F−N plot. All of the measured and calculated relevant parameters are listed in Table 1.

From Figure 1, we find that except for the tip structure other experimental parameters such as d, h, and r are almost the same and can be obtained accurately from the TEM image as shown in Figure 1c, so the change in electron field-emission characteristics results mainly from changes in the tip structure of the CNT. For a single CNT with a sharp tip, the field conversion factor is usually taken as $\beta = 1/kr$, where r is the radius of the tip and the empirical correction factor, k, is usually taken as $k \approx 5$ for a hemisphere on a cylinder.[6] However, in real situations the field strength also depends on the tip structure and the extractor distance (especially when it is very small). Values of k can be calculated from the $1/\beta$ values listed in Table 1. For the CNT shown in Figure 1, the radii of the capped and opened CNTs are both 8.0 nm, and k is found to be 1.72 and 1.37, respectively, for the capped (Figure 1d) and opened (Figure 1e) CNT. Here we use the value α to express the ratio $\beta_{open}/\beta_{close}$, and for the CNT shown in Figure 1 we have $\alpha = 1.26$.

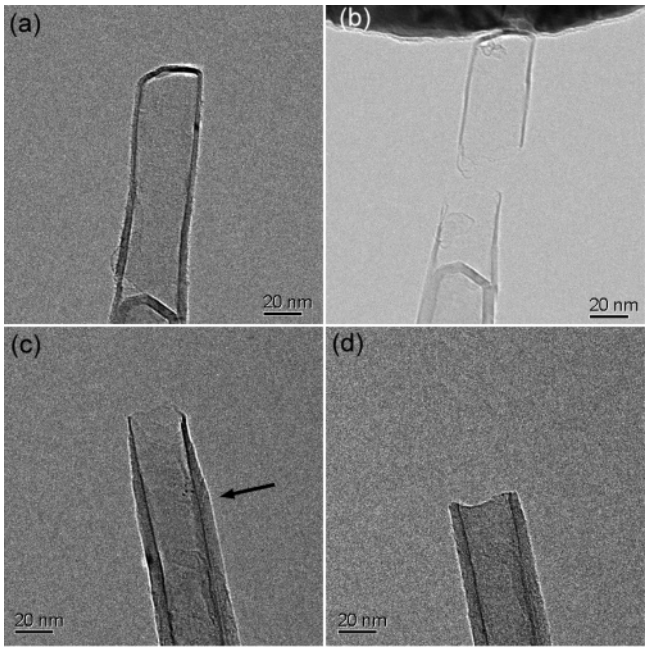

Figure 2. Cap of a close-ended CNT (a) was removed by current cutting (b). An open-ended CNT obtained by current cutting (c) was shortened by electrically-driven vaporization (d), and the arrow in c indicates the new tip position of d.

Because of the different tip structures, especially those of the opened CNT, different values of α are found for for different CNTs. Another comparison is shown in Figure 2a and b. The CNT was cut by large current near its closed end. Although the CNT was shortened by about 70 nm, relative to its length of more than 1 μm, the reduction in its length and hence in field enhancement can be neglected. The very thin (less than 1 nm) and irregular open end showed a much lower onset voltage than the closed one. In this case $\alpha = 1.50$, and in other cases this value could be more than two. In fact, all of our similar comparisons show that the open-ended CNTs have a higher field conversion factor and hence a lower onset voltage than closed CNTs.

The above results also seem to indicate that an open-ended CNT with a thinner wall is more favorable for emitting electrons than a thicker one. Figure 2c and d shows a direct comparison of two types of open-ended CNTs. The open-ended CNT in Figure 2c was obtained by current cutting, leaving a convex termination with a sharp edge of about 1 nm. After field-emission measurements, the above electrically-driven vaporization phenomenon (also see Figure 1e) was used to shorten the

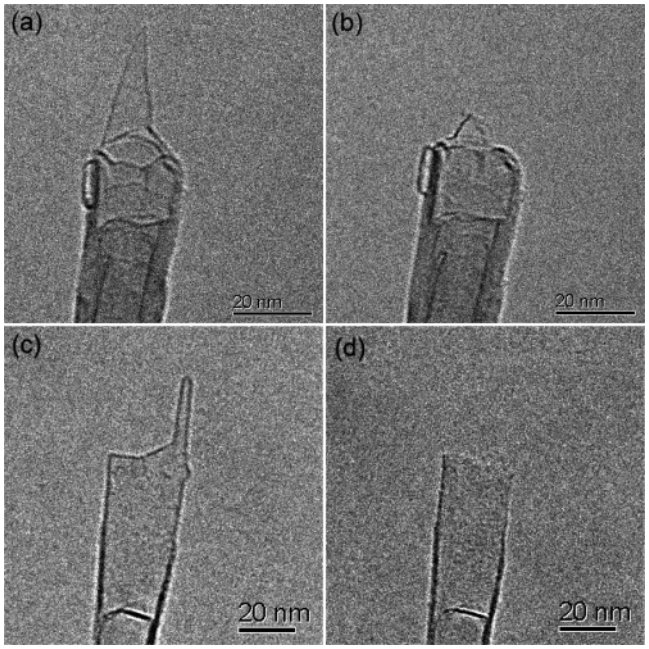

Figure 3. Nanotube before (a) and after (b) the removal of a triangular graphitic sheet on its end. (c) An occasionally obtained CNT with a thin capped CNT on its tip and the removal of this thin CNT leaving an open end (d).

CNT by about 50 nm, leaving a flat termination with a thicker wall of about 4.5 nm. The thinner CNT (Figure 2c) shows a lower onset voltage, V_{onset}, than a thicker CNT (Figure 2d). Using the data listed in Table 1 we have $\alpha = \beta_{thin}/\beta_{thick} = 1.33$. Mayer et al.[19] concluded from their calculation that MWCNTs with a convex termination are better emitters than those with flat terminations because a convex termination may result in a deeper field penetration into the potential barrier and therefore an increase in the emission current. In addition, we would like to emphasize that the open-ended CNTs (e.g., Figure 2b and c) are far from an ideal open-ended CNT with a circular edge. A careful examination of Figure 2b and c revealed that the tube wall near the tip did not have a simple circular edge structure. Instead the tip may better be regarded as being composed of irregular-shaped graphitic sheets, which may have more dangling bond states on their edges than on the flat edge of the usual CNT, and as pointed out by Tada and Watanabe[20] it is these dangling bond states that are most efficient in contributing to the emission current due to, among other things, better coupling with the states of the emitted electrons in the vacuum.

One of the most disputed results on the electron field-emission of CNTs is concern with the effect of the cap of the CNT. Although Bonard et al.[21] concluded that opened MWCNTs emit at about twice the voltage than that of closed MWCNTs, Rinzler et al.[7] found that the situation is opposite; that is, opened MWCNTs begin to emit electrons at less than half the onset voltage of closed MWCNTs. All of our observations support the results of Rinzler et al.; that is, opened CNTs are more efficient than closed CNTs in electron field-emission.

In our experiments, the field-emission properties of some "irregular" tip structures are also studied. Shown in Figure 3a is a CNT with a triangular-shaped graphitic sheet protruding from its open end, and this structure was often obtained after current cutting. Understandably, this extremely sharp tip results in an extremely low onset voltage of less than 28 V. When the graphitic sheet was removed under high field-emission current (more examples could be found in our previous work[10]), we found that the onset voltage increased by more than 100% from

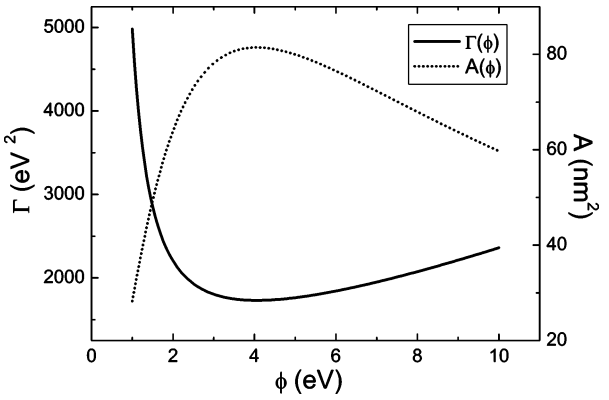

Figure 4. Calculated $\Gamma(\phi)$ and $A(\phi)$ as a function of ϕ for sample 1.

Figure 3a to b. Another example was shown in Figure 3c, where a strange finger structure was obtained occasionally. Instead of being a graphitic sheet, the protruding part was a thin capped CNT. This protruding CNT may be removed at high current leaving an open end. However, in this case the opened CNT (Figure 3d) is less efficient than the closed CNT (Figure 3c), which may be attributed to the much smaller diameter of the protruding closed CNT (Figure 3c). So our earlier conclusion that an opened CNT is more efficient than a closed CNT should be applied to CNTs with about the same diameters.

We now compare the onset local field of different tip structures, which is described by $F_{onest} = \beta V_{onset}$. Most values are around 4 V/nm (see Table 1), which is in good agreement with that of Bonard et al.[5] However, for some structures this value is close to 5 V/nm (e.g., sample 9 of Table 1, Figure 3c) or even larger. In examining the calculated emission area, A, of Table 1, we found that the smaller the emission area, the larger the F_{onest} is. Equation 1 shows that the larger the local field, F, the larger the current density, J (for a fixed ϕ), and it is understandable that to obtain the same emission current (e.g., $I = 1$ nA), the smaller emission area will result in a higher F_{onest} value. For sample 9, the calculated emission area is only about 4 nm^2, which is much smaller than other samples, and therefore a higher F_{onest}. In addition, the emission current, I, is more sensitive to the local field than the emission area, which is manifested in the comparison of samples 7 and 9, where a change in F_{onest} of 1 V/nm causes a change in emission area of more than 2 orders of magnitude.

In fact, the calculated emission area is very sensitive to the slope of the F−N plot (or field conversion factor). To reduce the error, each $I-V$ curve was obtained by an average of tens of sweep cycles and the F−N line was carefully fitted. However, the calculated emission area usually does not agree well with that of the actual tip size as shown in the TEM image. Nevertheless, certain general trends may still be found from our data.

For sample 1 (Figure 1d) the actual size of the CNT tip is at least πr^2, that is, about 200 nm^2, while the fitted emission area is only about 80 nm^2, suggesting that only part of the cap contributes effectively to the emission current. In fact, except for few cases nearly all of the closed CNTs (see, e.g., samples 3 and 9) show a smaller calculated emission area (some are much smaller) than the actual one.

For open-ended CNTs the situation is more complicated. The calculated emission areas are sometimes smaller (samples 2, 5, and 6), but in other other cases they are larger than the actual areas (samples 4, 7, 8, and 10). For sample 7 (Figure 3a), the onset voltage is extremely low. By assuming that the onset field emission was resulted from the very top of the protruding

graphitic sheet, the emission area is expected to be at most several square nanometers and even if considering the edge, the emission area is at most several tens of square nanometers, which is still much smaller than the calculated value of 470 nm^2, suggesting that the F−N analysis of the emission data for such a small emission tip might be not valid. For samples 4 and 10, both having very thin and sharp edges, the calculated emission areas are also much larger than expected.

Many people have noted that the standard F−N theory for a planar electrode does not give accurate results for emission from an extremely curved surface. For example, Edgcombe[22] pointed out recently that because of the extremely curved surface and the change in image force the potential distribution should be very different from that of a planar surface. In addition, the WKB approximation used in the F−N theory is not suitable for the highly inhomogeneous potential caused by a very sharp tip (e.g., ~1 nm diameter).[20] The graphitic sheets on the open end of a CNT usually show very sharp edges or irregular atomic protrusions. We believe that at this scale the standard F−N theory does not apply well, resulting in a large error in the calculation of the emission area.

However, most of the F−N plots obtained from our experimental field-emission $I-V$ curves follow a straight line shape, indicating that the top of the potential image-reduced barrier has not been pulled down below the Fermi level of the CNT and the electron emission process is still dominated by the tunneling of electrons from the CNT into the vacuum. The shape of the barrier is expected to have significant influence on the field-emission behavior and therefore the calculated emission area. In fact, compared with the simple triangular barrier ($\upsilon(y) = 1$) the image charge correction ($\upsilon(y) < 1$) does reduce the calculated emission area by a factor of 100.[16,23] Similarly, the shape of the barrier around the very sharp tip will be further changed and the function $\upsilon(y)$ should also be modified; therefore, the calculated emission area might be reduced to a reasonable value.

Other approximations of $t(y)$ and $\upsilon(y)$ have also been proposed by Charbonnier and Martin[24] (CM) giving $t(y) = 1.044$ and $\upsilon(y) = 0.956-1.062y^2$ (yet another similar approximation was proposed later by Spindt et al.[25]). Substituting these expressions into eqs 4−6, we obtain

$$s(y) = 0.956, \quad \beta = -0.956b\phi^{3/2}/S \tag{11}$$

and

$$R = \ln(Aa\beta^2/1.09\phi) + 10.45/\phi^{1/2} \tag{12}$$

The calculated results using eqs 11 and 12 are also listed in Table 1 (superscript as ^{CM}), and we can find some differences between results obtained by using the two methods. The CM approximation is suitable only in a certain current density range ($10 \le J \le 10^4 A/cm^2$)[24] and our experimental data used for calculations were obtained in a higher range ($10^4 \le J \le 10^6 A/cm^2$). Contrarily, the HK approximation[6,18] is sufficiently accurate in the whole possible current density range (or, equivalently, field range). We therefore believe that the results obtained using the HK approximation are more reliable. However, $s(y)$ in the CM approximation is a constant; hence, we do not need to calculate β by iterative approach, and the calculation of eq 12 is much more convenient. Furthermore, we found that the differences between results obtained using the two different methods are not very large, and the CM approximation therefore provides a good reference and quick estimation.

All of the above calculations were based on the assumption that the work function of the CNT is 5 eV. Different values of ϕ were reported for different samples and attributed to different synthesize and measurement methods. In our work, when we compare field conversion factors β of different tip structures, we do not have to know the exact work function of our samples. The measurements were carried out on the same CNT, and the work function of the same CNT should not change much. Recently, Xu et al. found that the work function at the tip of the CNT does depend on its structure and surface condition.[11] However, from their data, we found that the change of the work function is less than 6%. Because $\beta = -bs(y)\phi^{3/2}/S$, in which $s(y)$ can be considered to be constant, the uncertainty in β is expected to be less than 9%, which is much smaller than the typical α ratio found in this study. We therefore believe that the results of the comparisons are still valid even when considering the possible variation in the work function.

For the same batch of nanotubes, we can assume that the work function does not change much. But for different nanotubes synthesized by different methods and groups, this value may vary from 1.3 eV[26] to 7.3 eV,[27] and this will have some influence on the calculated emission area. If we substitute eq 8 into eq 9, we can get a formula for the emission area

$$A = e^R S^2/ab^2\Gamma \tag{13}$$

and the function

$$\Gamma = s^2(y_0)\, t^{-2}(y_0)\, \phi^2 \exp(-0.845 y_0^{1.69} S/s(y_0)V_0) \tag{14}$$

is the so-called emission area extraction function.[16] Because y_0 is also a function of ϕ, Γ has only one variable ϕ if S and V_0 are fixed. The function $\Gamma(\phi)$ and emission area $A(\phi)$ of sample 1 are plotted using eqs 14 and 13 in Figure 3 for $\phi = 1$ to $\phi = 10$. If a fixed value of $\Gamma(\phi) = 1910$ is chosen, we have $A(\phi) = 73.8\ nm^2$, and the error in the calculated emission area is not greater than ±10% (an accuracy of 10% is usually sufficient in practice[24,25]) over the range from $\phi = 2.15$ eV to 8.2 eV. In fact, the emission area obtained using $\phi = 5$ eV will not cause error greater than ±10% over the range from $\phi = 2.4$ eV to 7.0 eV (the results of other samples are similar). To our knowledge, except for a few extreme cases, this nearly covers the measured work-function range of carbon nanotubes. Our results are very similar to CM and Spindt's results obtained by their approximations.[24,25] However, their results are only suitable in some current density range. The accurately tabulated Γ in all ranges have been given by Forbes.[16] The middle of our current density range is $10^5\ A/cm^2$, and we found our calculations are in good agreement with Forbes's results.

The above calculations show that we can readily estimate the emission area using $\phi = 5$ eV without causing much error. Moreover, it also confirms that the large differences between the calculated emission area and observed size were not caused by uncertainty in the work function.

IV. Conclusions

In summary, individual carbon nanotubes with different tip structures were created in-situ by precise and controllable manipulation inside TEM. The field-emission properties were directly correlated with the tip structures. It was found that the field-emission characteristics of a CNT depend sensitively on its tip structure and field conversion factor may change for more than 100%. Open-ended CNTs show lower onset voltages than close-ended CNTs, and the irregular shaped graphitic sheets at the tip of the open-ended CNT may enhance the field emission

of the CNT remarkably. For some open-ended CNTs with atomic sharp edges, the standard F−N equation may no longer be valid and will need some modifications.

Acknowledgment. We are grateful to the support by the Ministry of Science and Technology (973 Grant no. 001CB610502, 863 Grant no. 2004AA302G11), National Science Foundation of China (Grant no. 10434010), the Chinese Ministry of Education (Grant nos. 10401 and 2004036178), and the National Center for Nanoscience and Technology of China.

References and Notes

(1) Dresselhaus, M. S.; Dresselhaus, G.; Avouris, Ph. *Carbon Nanotubes: Synthesis, Structure, Properties, and Applications*; Springer: New York, 2001.

(2) de Jonge, N.; Lamy, Y.; Schoots, K.; Oosterkamp, T. H. *Nature* **2003**, *420*, 393.

(3) de Heer, W. A.; Chatelain, A.; Ugarte, D. *Science* **1995**, *270*, 1179.

(4) Collins, P. G.; Zettl, A. *Appl. Phys. Lett.* **1996**, *69*, 1969.

(5) Bonard, J. M.; Dean, K. A.; Coll, B. F.; Klinke, C. *Phys. Rev. Lett.* **2002**, *89*, 197602.

(6) de Jonge, N.; Bonard, J. M. *Philos. Trans. R. Soc. London, Ser. A* **2004**, *362*, 2239.

(7) Rinzler, A. G.; Hafner, J. H.; Nikolaev, P.; Lou, L.; Kim, S. G.; Tomanek, D.; Nordlander, P.; Colbert, D. T.; Smalley, R. E. *Science* **1995**, *269*, 1550.

(8) Saito, Y.; Hamaguchi, K.; Hata, K.; Uchida, K.; Tasaka, Y.; Ikazaki, F.; Yumura, M.; Kasuya, A.; Nishina, Y. *Nature* **1997**, *389*, 554.

(9) Wang, Z. L.; Gao, R. P.; de Heer, W. A.; Poncharal, P. *Appl. Phys. Lett.* **2002**, *80*, 856.

(10) Wang, M. S.; Peng, L. M.; Wang, J. Y.; Chen, Q. *J. Phy. Chem. B* **2005**, *109*, 110.

(11) Xu, Z.; Bai, X. D.; Wang, E. G.; Wang, Z. L. *Appl. Phys. Lett.* **2005**, *87*, 163106.

(12) Wang, M. S.; Wang, J. Y.; Jin, C. H.; Chen, Q.; Peng, L. M. *Mater. Sci. Forum* **2005**, *475*−*479*, 4071.

(13) Purcell, S. T.; Vincent, P.; Journet, C.; Thien Binh, V. *Phys. Rev. Lett.* **2002**, *88*, 105502.

(14) Wang, M. S.; Wang, J. Y.; Chen, Q.; Peng, L. M. *Adv. Funct. Mater.* **2005**, *15*, 1825.

(15) Fowler, R. H.; Nordheim, L. *Proc. R. Soc. London, Ser. A* **1928**, *119*, 173.

(16) Forbes, R. G. *J. Vac. Sci. Technol., B* **1999**, *17*, 526.

(17) Houston, J. M. *Phys. Rev.* **1952**, *88*, 349.

(18) Hawkes, P. W.; Kasper, E. *Principles of Electron Optics II: Applied Geometrical Optics*; Academic: London, 1996.

(19) Mayer, A.; Miskovsky, N. M.; Cutler, P. H. *Phys. Rev. B* **2002**, *65*, 155420.

(20) Tada, K.; Watanable, K. *Phys. Rev. Lett.* **2002**, *88*, 127601.

(21) Bonard, J. M.; Kind, V.; Stockli, T.; Nilsson, L. O. *Solid-State Electron.* **2001**, *45*, 893.

(22) Edgcombe, C. *J. Phys. Rev. B* **2005**, *72*, 045420.

(23) Edgcombe, C. J.; Valdre, U. *Solid-State Electron.* **2001**, *45*, 857.

(24) Charbonnier, F. M.; Martin, E. B. *J. Appl. Phys.* **1962**, *33*, 1897.

(25) Spindt, C. A.; Brodie, I.; Humphrey, L.; Westerberg, E. R. *J. Appl. Phys.* **1976**, *47*, 5248.

(26) Gulyaev, Y. V.; Sinitsyn, N. I.; Torgashov, G. V.; Mevlyut, Sh. T.; Zhbanov, A. I.; Zakharchenko, Yu. F.; Kosakovskaya, Z. Ya.; Chernozatonskii, L. A.; Glukhova, O. E.; Torgashov, I. G. *J. Vac. Sci. Technol., B* **1997**, *15*, 422.

(27) Fransen, M. J.; van Rooy, T. L.; Kruit, P. *Appl. Surf. Sci.* **1999**, *146*, 312.